A Succession of Mechanisms Stimulate Efficient Reconstituted HIV-1 Minus Strand Strong Stop DNA Transfer†

Min Song,‡,¶ Mini Balakrishnan,‡,§ Robert J. Gorelick,|| and Robert A. Bambara*,‡

Department of Biochemistry and Biophysics, University of Rochester, Rochester, New York 14642, and AIDS and Cancer Virus Program, SAIC Frederick, Inc., National Cancer Institute-Frederick, P.O. Box B, Frederick, Maryland 21702-1201

Received November 21, 2008; Revised Manuscript Received January 9, 2009

ABSTRACT: Donor−acceptor template systems in vitro were designed to test mechanisms of minus strand transfer of human immunodeficiency virus 1 (HIV-1). Donor RNA D199, extending from the 5′ end of the HIV-1 genome to the primer binding site (PBS), promoted transfer to only 35% with an acceptor RNA representing the 3′ terminal 97 nucleotides, whereas donor RNA D520, including an additional 321 nucleotides 3′ of PBS, exhibited 75% transfer. Both donors transferred through an invasion-driven pathway, but transfer was stimulated by the folding structure resulting from the extra segment in D520. In this study, the significance of interaction between the $tRNA^{lys3}$ primer and U3 was examined. Measurements utilizing acceptors having or lacking the U3 region complementary with $tRNA^{lys3}$ indicated that a $tRNA^{lys3}$−U3 interaction compensated for inefficient acceptor invasion observed with D199. Stimulation presumably occurred because binding to $tRNA^{lys3}$ increased the proximity of the acceptor to elongated cDNA, improving transfer to 78% efficiency with D199, and even higher to 85% with D520. The stimulation did not require natural viral sequences but could be achieved by substituting the original U3 sequence with an equal length sequence that binds a different region of $tRNA^{lys3}$. Comparison between acceptors sharing the natural region for $tRNA^{lys3}$−U3 interaction but having or lacking the acceptor invasion site demonstrated that $tRNA^{lys3}$−U3 interaction and acceptor invasion cooperate for maximal stimulation. Overall, observations suggest that both proximity and invasion mechanisms are applied successively by HIV-1 for efficient minus strand transfer.

During retroviral replication, single-stranded viral genomic RNA is converted into double-stranded viral DNA by the virus-encoded enzyme reverse transcriptase (RT),[1] in the pathway termed reverse transcription (*1, 2*). Reverse transcription of retroviruses, including HIV-1, is initiated by a virion-packaged cellular tRNA primer annealed to the PBS located near the 5′ end of genomic RNA. RT-catalyzed DNA synthesis proceeds toward the 5′ end of the viral genome, generating the 199-nucleotide minus strand strong stop DNA (−sssDNA). Meanwhile, the RNase H activity of the RT makes endonucleolytic cleavages on the copied RNA genome, facilitating the −sssDNA to translocate from the 5′ repeat (R) region of the viral genome to the 3′ R. This step is termed −sssDNA transfer. Minus strand DNA synthesis then resumes through a series of steps to produce full-length double-stranded DNA (*3, 4*).

Extensive studies have demonstrated that nucleocapsid protein (NC) significantly stimulates minus strand transfer in vitro (*5*). NC is a nucleic acid chaperone (*6, 7*). It was suggested that NC enhances the rate of annealing between complementary nucleic acid strands, more specifically, the annealing between −sssDNA and 3′ end of the viral genome through R region complementarity during minus strand synthesis and transfer (*8*−*12*). Also, it was reported that NC inhibits DNA self-priming of the −sssDNA, a pathway leading to a dead-end product, in a manner that greatly improves transfer (*10, 11, 13*−*17*).

Reconstituted systems in vitro, with donor RNA templates representing the 5′ end of the viral genome and acceptor RNA templates representing the 3′ end of the viral genome, were designed and used to probe possible mechanisms of HIV-1 minus strand transfer (*18*−*24*). When the homology between donor and acceptor RNAs consisted of only a short segment of the 5′-most sequence on the donor, RT RNase H cleavages at the very end of the donor facilitated the dissociation of −sssDNA from the donor and transfer to the acceptor (*25*−*28*), a mechanism termed the terminus transfer pathway (*19, 22*). When the level of homology between donor and acceptor was greater, RNase H cleavages occurring early in the primer extension reaction generated gaps in the donor (*29*), promoting the acceptor to invade and hybridize to the cDNA (*30*). A region at the base of the trans-

† This work was supported by National Institutes of Health Grant GM049573 (to R.A.B.).

* To whom correspondence should be addressed: Department of Biochemistry and Biophysics, University of Rochester Medical Center, 601 Elmwood Ave., Box 712, Rochester, NY 14642. Telephone: (585) 275-3843. Fax: (585) 275-6007. E-mail: robert_bambara@urmc.rochester.edu.

‡ University of Rochester.

§ Present address: Gilead Sciences, 333 Lakeside Dr., Foster City, CA 94404.

¶ Present address: Stanford University School of Medicine, 300 Pasteur Drive, Stanford, CA 94305-5120.

|| National Cancer Institute-Frederick.

[1] Abbreviations: HIV-1, human immunodeficiency virus, type 1; PBS, primer binding site; NC, nucleocapsid; nt, nucleotide(s); R, repeat; RT, reverse transcriptase; −sssDNA, minus strand strong stop DNA; DIS, dimerization initiation sequence.

10.1021/bi802149j CCC: $40.75
Published on Web 02/04/2009

activation-responsive (TAR) hairpin was particularly effective at pausing RT synthesis, allowing the RNase H to clear an area thought to be the primary invasion site. The acceptor−cDNA hybrid then propagated, finally reaching the cDNA 3′ terminus, which transferred to complete the reaction. This mechanism has been termed the acceptor invasion-driven pathway (*20, 21, 23*). Additionally, we recently designed experiments showing that as a result of successful acceptor invasion, the increased local concentration of complementary acceptor sequences at the cDNA 3′ terminus facilitated direct transfer through a proximity mechanism (*24*).

In retroviruses, a host-encoded tRNA is utilized as the primer by RT to initiate −sssDNA synthesis (*4*). Some retroviruses can readily be mutated to use an alternative type of tRNA. It was observed that murine leukemia viruses (MLV) harboring specific mutations in the PBS matching the 3′ end of alternative tRNA primers replicated with no great difference in efficiency in vivo. This suggested that the PBS−tRNA primer complementarity rather than features of the unique natural tRNA primer is essential for facile replication of MLV (*31, 32*). With HIV-1, although various primers could be utilized in reconstituted systems in vitro (*33*), the natural $tRNA^{lys3}$ conferred a substantial advantage in vivo. In contrast to what was observed with MLV, different PBS−tRNA primer combinations in HIV-1 led to significant lags in viral replication. These observations suggest that the natural $tRNA^{lys3}$ makes unique contacts that are essential for optimal viral growth of HIV-1 (*34*−*37*).

Several studies have demonstrated that interactions between tRNA and the viral genome outside of PBS are important for retroviral replication (*33, 38*−*46*). For instance, it was suggested that for avian sarcoma and leucosis virus, an interaction between the TψC loop of the $tRNA^{trp}$ and the U5 region of viral genomic RNA is essential for efficient initiation of reverse transcription (*38*). For HIV-1, $tRNA^{lys3}$ is capable of interacting with viral genomic RNA at multiple sites (*47, 48*). The interaction between the anticodon loop of $tRNA^{lys3}$ and the A-rich loop upstream of PBS in the viral genome is essential for replication of HIV-1 (*49*), and additional interactions between $tRNA^{lys3}$ and the viral genome are supported by structure probing analysis of the $tRNA^{lys3}$−genomic RNA binary complex (*48*). In addition, it was observed that the anticodon loop and the D-loop of $tRNA^{lys3}$ interact with HIV-1 RT (*50*−*52*), and such $tRNA^{lys3}$−RT interaction stimulates both the DNA polymerase and RNase H activity of RT (*53*). Moreover, the unwinding of the highly structured $tRNA^{lys3}$ primer is promoted by NC. It was suggested that NC facilitates the interaction of the $tRNA^{lys3}$ primer with the PBS to initiate reverse transcription (*54*). The overall results indicate that interactions of $tRNA^{lys3}$ with RT, NC, and the viral genome outside of PBS are essential for replication of HIV-1 (*47*−*55*).

Previously in a DNA-primed transfer reaction in vitro, we showed that donor RNA D199, which included the minimal region required for minus strand synthesis, promoted transfer to only 35% with an acceptor RNA named A97h. This acceptor was homologous to the 5′-most 97 nucleotides of the donor. The sequence includes the putative invasion site at the base of the TAR hairpin and therefore allows invasion-driven transfer. Donor RNA D520, which included an additional 321 nt 3′ of PBS, transferred at an efficiency of 75%. We determined that both donors promoted transfer primarily through the invasion-driven pathway (*23*). For D520, however, the folding configuration of the longer donor promoted much more effective invasion and terminus transfer. We also found evidence that efficient acceptor invasion increases the local concentration of the acceptor for effective transfer through a second proximity effect pathway in addition to the originally conceived branch migration pathway of propagation (*24*).

Marquet and co-workers proposed that interaction of the $tRNA^{lys3}$ primer with U3 greatly enhanced minus strand transfer of HIV-1 in vitro. It was observed that a nonanucleotide segment, at positions 9091−9099 in the U3 region of the Mal strain of HIV-1, is exactly complementary to nucleotides 38−46 of $tRNA^{lys3}$ (Figure 1). In a $tRNA^{lys3}$-primed transfer reaction, there was a significant decrease in the level of transfer when using acceptors in which that nonanucleotide segment was mutated or deleted. This implies that the $tRNA^{lys3}$−U3 interaction contributes to more efficient transfer during viral replication (*56*). Since the nonanucleotide segment in U3 identified by the Marquet group is well-conserved throughout different strains of HIV-1 (*56*), we investigated whether such $tRNA^{lys3}$−U3 interaction (*56*) could also influence transfer in our D520 and D199 systems. The approach was to modify our systems to prime with $tRNA^{lys3}$ and compare transfer efficiency when the acceptors had or lacked the nonanucleotide segment. We were particularly interested in determining how the $tRNA^{lys3}$−U3 interaction influences invasion-driven transfer and whether the extra sequences in D520 would synergize with the U3 sequences to maximize transfer efficiency.

MATERIALS AND METHODS

Materials. Recombinant HIV-1 reverse transcriptase (p66/p51 heterodimer) was purified as described previously (*57, 58*). HIV-1 NC (71 amino acids) was prepared as described previously (*59, 60*). DNA oligonucleotides were purchased from Integrated DNA Technologies, Inc. (IDT, Coralville, IA). The pNL4-3 molecular clone was obtained through the AIDS Research and Reference Reagent Program (Division of AIDS, National Institute of Allergy and Infectious Diseases, National Institutes of Health, Bethesda, MD). The T7-MEGAshortscript high-yield transcription kit was purchased from Ambion, Inc. (Austin, TX). The Platinum *Taq* DNA polymerase was purchased from Invitrogen (Carlsbad, CA). The purified $tRNA^{lys3}$ from human placenta was purchased from Bio S&T (Lachine, QC). The ^{32}P isotope was purchased from Perkin-Elmer Life Science (Boston, MA). All other enzymes as well as the dNTP mixture were purchased from Roche Applied Science (Indianapolis, IN).

Preparation of Donor and Acceptor RNA Substrates. Genomic sequences of the HIV-1 pNL4-3 strain were amplified by PCR using *Taq* DNA polymerase to generate DNA templates for the preparation of RNA samples. The donor RNA templates D199, D520 and acceptor RNA template A97h, A19h were generated by runoff transcription in vitro as described previously (*23, 24*). The acceptor RNA substrates A97h(−54), Δ-A97h(−54), mut-A97h(−54), A19h(−54), and mat-A97h(−54) were transcribed in vitro from a synthetic double-stranded DNA fragment using the Ambion T7-MEGAshortscript kit. The sequence of the

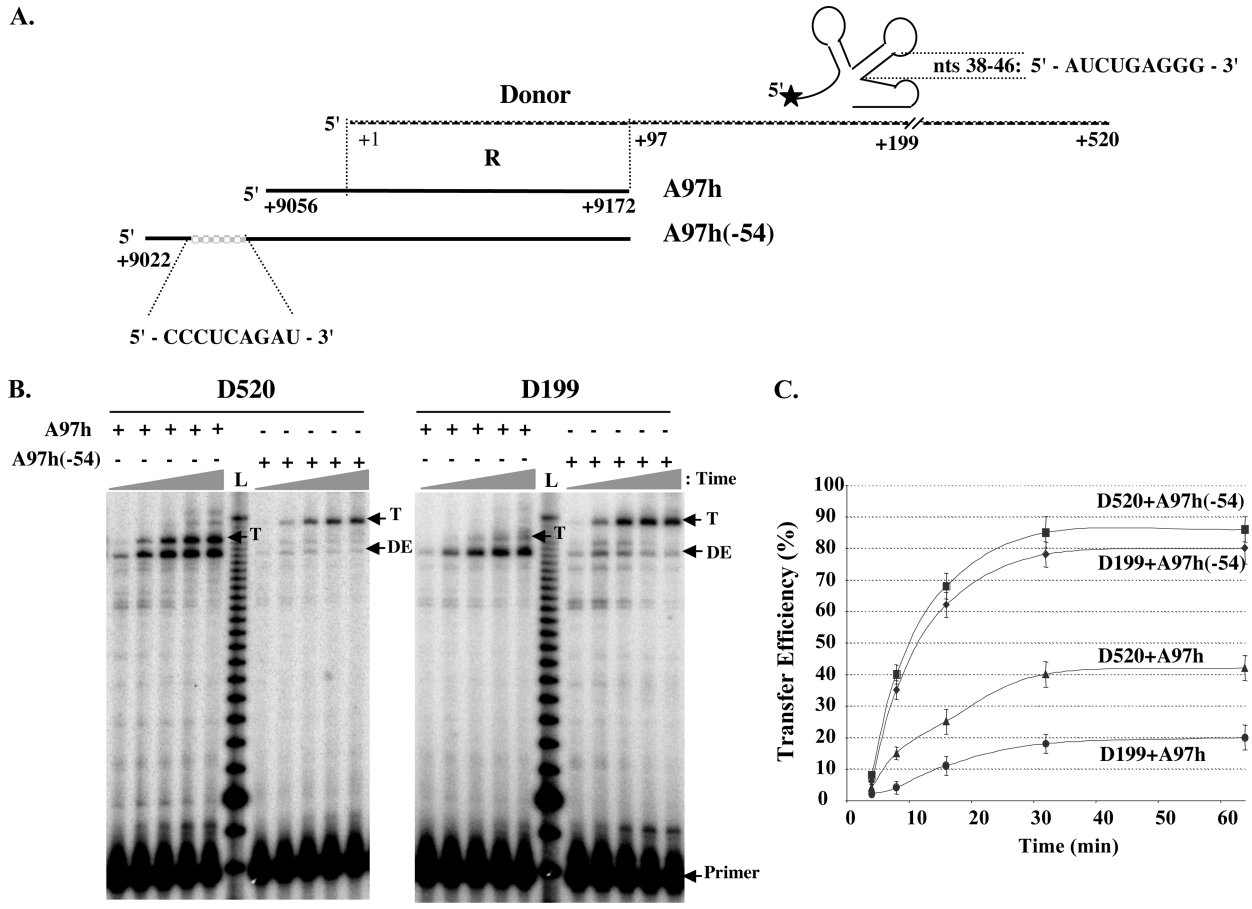

FIGURE 1: Analysis of the $tRNA^{lys3}$−U3 interaction during an acceptor invasion-driven transfer reaction based on the NL4-3 strain of HIV-1 genomic RNA. (A) Schematic of the experimental design. Donor D199 spans the 5′ R, U5, and PBS. Donor D520 contains the 520 nt of the 5′ end of the genomic sequence. Acceptor A97h shares 97 nt of homology with the donor RNAs and contains 20 nt of the U3. Acceptor A97h(−54) shares 97 nt of homology with the donor RNAs and contains a 54 nt segment extension into U3. The nonanucleotide sequence 5′-CCCUCAGAU-3′ (patterned line) complementary to nt 38−46 of $tRNA^{lys3}$ is included in the U3 region of A97h(−54). This nonanucleotide sequence occurs at positions 9091−9099 in the Mal strain of HIV-1 and positions 9033−9041 in the NL4-3 strain of HIV-1. (B) Transfer reaction mixtures with either A97h or A97h(−54) were sampled at 4, 8, 16, 32, and 64 min. Transfer products (T) and donor extension products (DE) are indicated. (C) Quantitative data showing transfer efficiencies of each reaction in a time-dependent manner. Results were plotted for the transfer reaction of D520 with A97h(−54) (■), D199 with A97h(−54) (◆), D520 with A97h (▲), and D199 with A97h (●). The transfer efficiency at each time point was calculated as 100% × T/(T + DE). Values were averaged from at least three independent experiments.

forward PCR primer for A97h(−54) was 5′-TAA TAC GAC TCA CTA TAG GGA GTG GCG AGC CCT CAG ATG-3′, whereas the sequence of the reverse primers for A97h(−54) was 5′-TGA AGC ACT CAA GGC AAG CTT TAT TGA GGC-3′. The sequence of the forward PCR primer for Δ-A97h(−54) was 5′-TAA TAC GAC TCA CTA TAG GGA GTG GCG AGG CTG CAT ATA AGC AGC TGC TTT TTG CCT GTA-3′, whereas the sequence of the reverse primers for Δ-A97h(−54) was 5′-TGA AGC ACT CAA GGC AAG CTT TAT TGA GGC-3′. The sequence of the forward PCR primer for mut-A97h(−54) was 5′-TAA TAC GAC TCA CTA TAG GGA GTG GCG AGT ATA TAT ATG CTG CAT ATA AGC AGC TGC TTT TTG CC-3′, whereas the sequence of the reverse primers for mut-A97h(−54) was 5′-TGA AGC ACT CAA GGC AAG CTT TAT TGA GGC-3′. The sequence of the forward PCR primer for A19h(−54) was 5′-TAA TAC GAC TCA CTA TAG GGA GTG GCG AGC CCT CAG ATG-3′, whereas the sequence of the reverse primers for A19h(−54) was 5′-GGT CTA ACC AGA GAG ACC CAG TAC AGG CA-3′. The sequence of the forward primer for mat-A97h(−54) was 5′-TAA TAC GAC TCA CTA TAG GGA GTG GCG AGA GTC TGA TGG CTG CAT ATA AGC AGC TGC TTT TTG CC-3′, whereas the sequence of the reverse primer for mat-A97h(−54) was 5′-TGA AGC ACT CAA GGC AAG CTT TAT TGA GGC-3′. In the NL4-3 strain of HIV-1, the nonanucleotide segment in U3 discovered by Marquet's group occupies positions 9033−9040. All RNA templates used in the study were purified by denaturing PAGE and resuspended in 10 mM Tris-HCl (pH 8.0), 1 mM EDTA buffer. RNAs were quantified by using the Ribogreen assay (Molecular Probes, Eugene, OR).

Preparation of 5′-Radiolabeled $tRNA^{lys3}$ Primer and DNA Primers. Preparation of 5′-radiolabeled $tRNA^{lys3}$ was performed as described previously with slight modifications (*61*). A 3-fold excess of a 38 nt DNA oligonucleotide template (UP5), having the sequence 5′-TG TGG AAA ATC TCT AGC AGT GGC GCC CGA ACA GGG AC-3′, was heat-annealed to $tRNA^{lys3}$ at 65 °C for 5 min in buffer consisting of 50 mM Tris-HCl (pH 8.0) and 75 mM KCl and gradually cooled to 37 °C. The reaction mixture was then treated with calf intestinal phosphatase (Roche) at 50 °C for 60 min, extracted with a phenol/chloroform mixture, precipitated with ethanol, and resuspended in 50 mM Tris-HCl (pH 8.0) and

75 mM KCl. Following incubation at 65 °C for an additional 5 min and slow cooling to 37 °C, the reaction mixture was treated with [γ-^{32}P]ATP [6000 (222TBq) Ci/mmol]. The radiolabeled tRNA^{lys3} and DNA template UP5 were separated by electrophoresis in a 6% sequencing gel. The tRNA^{lys3} template was eluted from the gel overnight, precipitated with ethanol, and resuspended in 10 mM Tris-HCl (pH 8.0), 1 mM EDTA buffer.

The sequence of DNA primer P1 is 5′-GCC CGG ATA GCT CAG ACG GAA GAG CAT CAG ACT CTT AAT CTG AGG GAC CAG GGT TCA AGT CCC TGT TCG GGC GCC A-3′. The sequence of DNA primer P2 is 5′-GTC CCT GTT CGG GCG CCA-3′. Preparation of 5′-radiolabeled DNA primers P1 and P2 was performed as described previously (*23, 24*).

Strand Transfer Assay. Reactions were performed as described previously with slight modifications (*23, 24*). The tRNA^{lys3} primer or DNA primers were heat-annealed to donor RNA via incubation at 65 °C for 5 min and slowly cooled to room temperature. Acceptor templates were then added and incubated with 150% NC (100% NC = 7 nt/NC) at 37 °C for 5 min. Primer, donor, and acceptor were mixed at a ratio of 1.5:1:3. RT was prebound to substrate at 37 °C for 5 min before reactions were initiated with $MgCl_2$ and dNTPs. Final reaction mixtures contained 50 mM Tris-HCl (pH 8.0), 50 mM KCl, 1 mM DTT, 1 mM EDTA, 32 nM HIV-1 RT, 6 mM $MgCl_2$, and 50 μM dNTPs. Reaction mixtures were incubated at 37 °C, and reactions were terminated at appropriate time points with 2× termination dye [10 mM EDTA (pH 8.0), 90% (v/v) formamide, and 0.1% each xylene cyanol and bromophenol blue]. Products were resolved by denaturing PAGE and analyzed using a PhosphorImager (GE Healthcare) and ImageQuant (version 2.1). Sizes of DNA products were estimated by using a 10 bp DNA ladder.

RESULTS

Interaction of tRNA^{lys3} with U3 Stimulates Minus Strand Transfer of both D520 and D199. To analyze how the interaction between tRNA^{lys3} and U3 affected the minus strand transfer of D520 and D199, RNA acceptor template A97h(−54) was designed and a 5′-radiolabeled tRNA^{lys3} primer was prepared (Figure 1A). A97h(−54) was identical to acceptor template A97h, used in previous work (*23, 24*), with an additional 34 nt extension into U3 to include the special nonanucleotide segment complementary to nt 38−46 of tRNA^{lys3}. Consequently, transfer products generated through acceptor A97h(−54) would be 34 nt longer than transfer products generated through acceptor A97h. For both of the transfer systems of D520 and D199, transfer products and donor extension products accumulated as the reaction proceeded when using acceptor template A97h (Figure 1B). Surprisingly, when acceptor template A97h(−54) was used, donor extension products accumulated until ∼16 min and then faded out as they were chased into transfer products during the transfer reaction of D199. Moreover, donor extension products were barely visible even in early time points with D520. Transfer efficiencies of D520 or D199 with each acceptor template are presented in Figure 1C in a graph of time dependence. All of the transfer reactions reached a plateau at 32 min. After the reactions were completed at that time, for donor D520, the transfer efficiency increased from 40% with A97h to 85% with A97h(−54); for donor D199, the transfer efficiency increased remarkably from 18% with A97h to 78% with A97h(−54). Clearly, the additional 34 nt extension in the U3 region of acceptor A97h(−54) promoted transfer in both of the donor systems. This result is in thorough agreement with discoveries described by the Marquet group (*56*). It shows that the interaction between tRNA^{lys3} and U3 promotes a transfer efficiency 2 times greater than that using A97h for D520, and the transfer improvement increases to 4 times for D199.

Deletion of the tRNA^{lys3}−U3 Interaction Inhibits Minus Strand Transfer. Another way to analyze the importance of tRNA^{lys3}−U3 interaction was to delete or mutate the nonanucleotide segment in U3 responsible for interaction with tRNA^{lys3} and determine the effects on transfer. RNA acceptor templates Δ-A97h(−54) and mut-A97h(−54) were designed (Figure 2A) for this purpose. Δ-A97h(−54) was generated by deleting the nonanucleotide segment from A97h(−54), and mut-A97h(−54) was generated by replacing the wild-type nonanucleotide sequence in A97h(−54) with base substitutions.

Figure 2B shows the transfer profile of D520 and D199 with each acceptor in a graph of time dependence. Clearly, the absence of the wild-type nonanucleotide segment in U3 led to a significant decrease in the degree of synthesis of transfer products for both donors. When we summarized the final efficiencies after each transfer reaction was completed (Figure 2D), we observed that for D520, the transfer efficiency decreased from 85% with A97h(−54) to 46% with Δ-A97h(−54) and to 29% with mut-A97h(−54). The decrease was even greater with D199. The transfer efficiency dropped from 78% with A97h(−54) to 28% with Δ-A97h(−54) and to 12% with mut-A97h(−54). This result further supports the conclusion that the presence of tRNA^{lys3}−U3 interaction is essential for efficient transfer of D520 or D199 with A97h(−54).

Interaction of tRNA^{lys3} with U3 and Acceptor Invasion-Driven Interaction Cooperate for Maximal Transfer. To examine whether the interaction of tRNA^{lys3} with U3 alone is sufficient to promote the highest transfer efficiency or it needs to work with acceptor invasion involved with A97h(−54) for maximal stimulation, two acceptor templates, A19h and A19h(−54), were designed (Figure 2A). A19h(−54) shared the same homologous region as A19h but included an extended U3 region which incorporated the nonanucleotide segment complementary to nt 38−46 of tRNA^{lys3}. Increases in the level of transfer with A19h(−54), as opposed to A19h, are likely imposed by the presence of elongated U3 in A19h(−54). Also, A19h(−54) shared the same U3 region as A97h(−54) but was homologous to the first 19 nt of the 5′ end of the donor templates, which could only allow for terminal transfer. Should any differences be observed in transfer ability between A19h(−54) and A97h(−54), they could be attributed to only an acceptor invasion-driven pathway involved with A97h(−54).

Figure 2C shows the transfer profile for each acceptor template with D199 or D520 in a graph showing time dependence, and the final transfer efficiencies after reactions were completed are summarized in Figure 2D. For D520, the transfer efficiency increased from 15% with A19h to 56% with A19h(−54), significantly lower than the value of 85% observed with A97h(−54). For donor D199, there was hardly

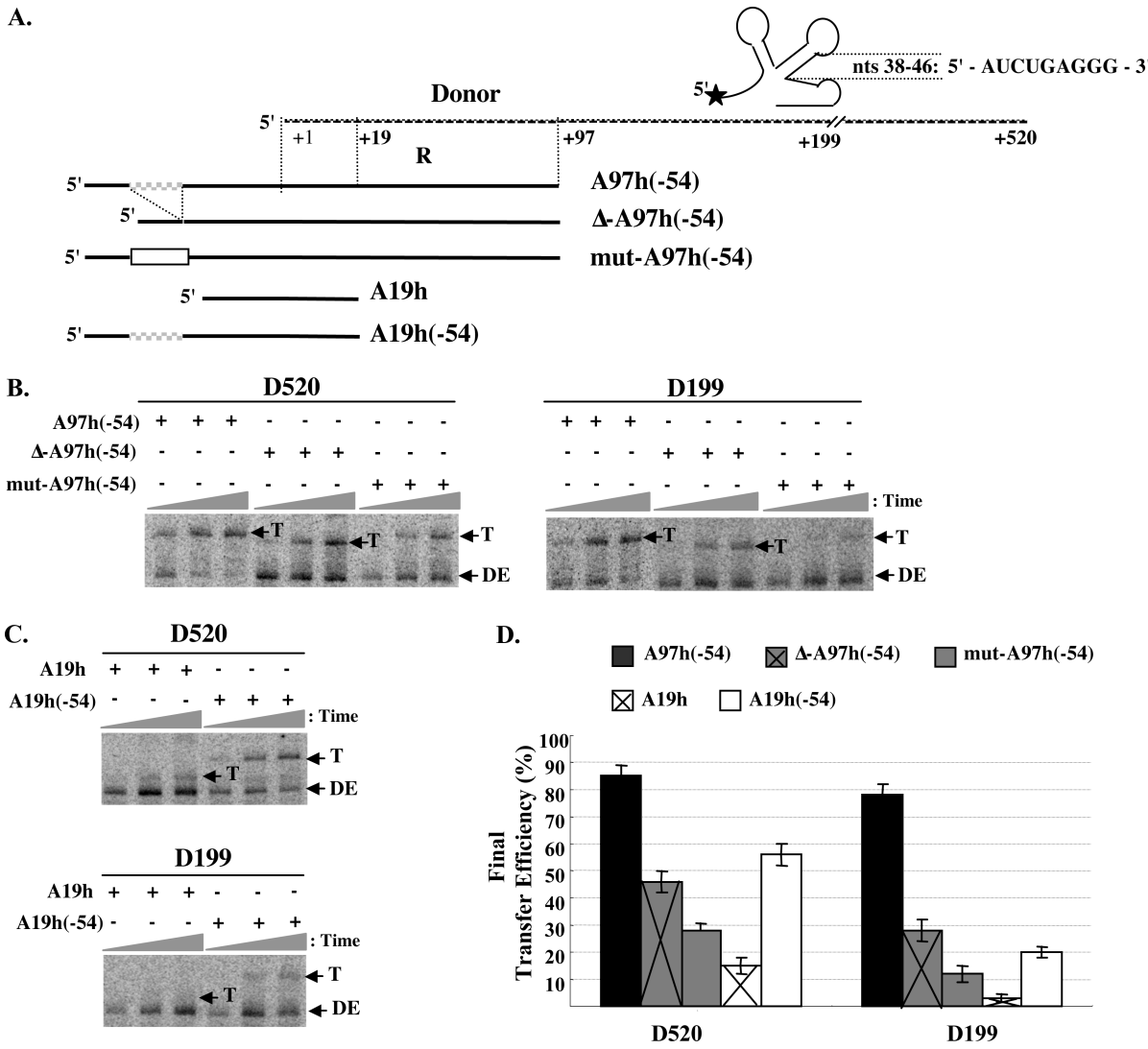

FIGURE 2: Effect of the $tRNA^{lys3}$−U3 interaction on minus strand transfer. (A) Schematic of the experimental design. Acceptor Δ-A97h(−54) was generated by deleting the nonanucleotide sequence 5′-CCCUCAGAU-3′‘ (patterned line) from U3 of wild-type A97h(−54). mut-A97h(−54) was generated by substituting the wild-type nonanucleotide sequence with alternative bases (empty box). Acceptor A19h is homologous to 19 nt at the 5′ terminus of the donor RNAs and contains 20 nt of U3. Acceptor A19h(−54) contains the same homology region as A19h and a 54 nt segment extension in U3 as A97h(−54). The nonanucleotide sequence 5′-CCCUCAGAU-3′ (patterned line) complementary to nt 38−46 of $tRNA^{lys3}$ is included in the U3 region of A19h(−54). (B) Transfer reaction mixtures were sampled at 10, 20, and 30 min. Transfer products (T) and donor extension products (DE) are indicated. (C) Quantitative data showing final transfer efficiencies of 30 min reactions. Transfer efficiencies with A97h(−54), Δ-A97h (−54), mut-A97h(−54), A19h, and A19h(−54) were plotted for D520 and D199. The transfer efficiency was calculated as 100% × T/(T + DE). Values were averaged from at least three independent experiments.

any transfer product throughout the reaction with A19h. The transfer efficiency increased from 2% with A19h to only 20% with A19h(−54). Evidently, compared to acceptor A19h, the presence of the extended U3 region in acceptor A19h(−54) promoted transfer for both of the donor systems through additional interaction with the $tRNA^{lys3}$ primer. More importantly, for both donors, the significant difference in transfer between using A19h(−54) and using A97h(−54) suggests that the interaction of $tRNA^{lys3}$ with U3 is not sufficient to promote the most efficient transfer. Overall, observations show that the invasion-driven interaction facilitated by A97h(−54) needs to cooperate with the interaction between $tRNA^{lys3}$ and U3 to achieve the maximal efficiency.

Alternative Sequence Interaction of $tRNA^{lys3}$ with U3 Also Promotes Efficient Minus Strand Transfer. To examine whether alternative stabilizing interactions between $tRNA^{lys3}$ and U3 can also facilitate more efficient transfer like the $tRNA^{lys3}$−U3 interaction suggested by the Marquet group (*56*), acceptor mat-A97h(−54) was designed (Figure 3A). The mat-A97h(−54) acceptor shared the same sequence as A97h(−54) except that the original nonanucleotide segment in U3 (5′-CCCUCAGAU-3′), complementary to nt 38−46 of $tRNA^{lys3}$, was substituted with a segment (5′-AGUCUGAUG-3′) complementary to nt 25−33 of $tRNA^{lys3}$. We anticipated that any improvement in transfer efficiency with mat-A97h(−54) would likely be imposed by the $tRNA^{lys3}$−U3 interaction conferred by the alternative sequence complementarity.

Figure 3B shows the transfer profile of D520 and D199 with acceptor mat-A97h(−54) in a graph of time dependence. The final transfer efficiencies are summarized in Figure 3C. After the transfer reactions were completed, D520 promoted an efficiency of ∼85% and D199 promoted an efficiency of

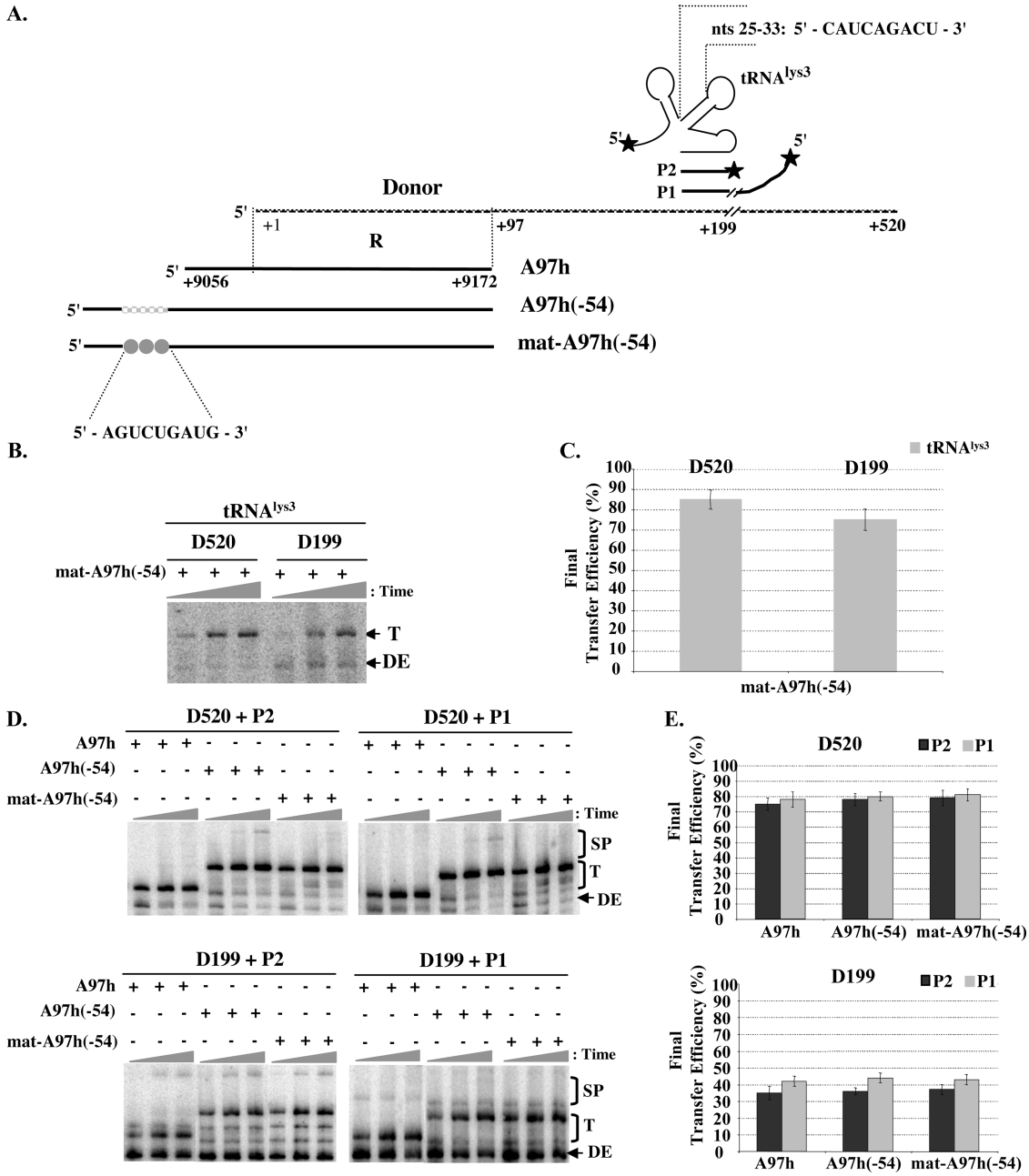

FIGURE 3: Effect of alternative primer−U3 interaction on minus strand transfer. (A) Schematic of the experimental design. Acceptors A97h and A97h(−54) are the same as those described in the legend of Figure 1. Acceptor mat-A97h(−54) is similar to acceptor A97h(−54) except that a nine-nucleotide segment (5′-AGUCUGAUG-3′) (circles) was substituted for the wild-type viral sequence (5′-CCCUCAGAU-3′). The nine-nucleotide mutation is complementary to nt 25−33 of $tRNA^{lys3}$. DNA primer P1 contains the same sequence as $tRNA^{lys3}$. DNA primer P2 contains the first 18 nt of the 3′ end of $tRNA^{lys3}$ and is complementary to PBS. (B) Transfer reaction mixtures of D520 and D199 with acceptor mat-A97h(−54) were sampled at 10, 20, and 30 min. Transfer products (T) and donor extension products (DE) are indicated. (C) Quantitative data showing final transfer efficiencies of 30 min reactions. The transfer efficiency was calculated as 100% × T/(T + DE). Values were averaged from at least three independent experiments. (D) P1- or P2-primed transfer reactions with either A97h, A97h(−54), or mat-A97h(−54). Each reaction mixture was sampled at 10, 20, and 30 min. Transfer products (T), donor extension products (DE), and self-priming products (SP) are indicated. (E) Quantitative data showing final transfer efficiencies of 30 min reactions. Transfer efficiencies with the P1-primed reaction (gray) and P2-primed reaction (black) were plotted for D520 and D199. The transfer efficiency was calculated as 100% × T/(T + DE + SP). Values were averaged from at least three independent experiments.

∼75%, almost to the same level as we observed previously when using acceptor A97h(−54). Clearly, the alternative sequence complementarity between mat-A97h(−54) and $tRNA^{lys3}$ contributed to more efficient transfer. Presumably, the interaction of mat-A97h(−54) with $tRNA^{lys3}$ brought the acceptor 5′ terminus closer to the elongated cDNA and facilitated more effective transfer through an acceptor proximity effect, a mechanism similar to that observed with A97h(−54). These results suggest that the $tRNA^{lys3}$−U3 interaction rather than the specific wild-type sequence of the substrates is the essential determinant for efficient minus strand transfer.

A DNA Primer with the Same Sequence as $tRNA^{lys3}$ Could Not Promote Efficient Minus Strand Transfer like $tRNA^{lys3}$. It was suggested that $tRNA^{lys3}$ folds into a secondary structure and interacts with HIV-1 genomic RNA at multiple positions (*48, 55, 62*). To examine whether the folding of $tRNA^{lys3}$ is important for the interaction with U3 that

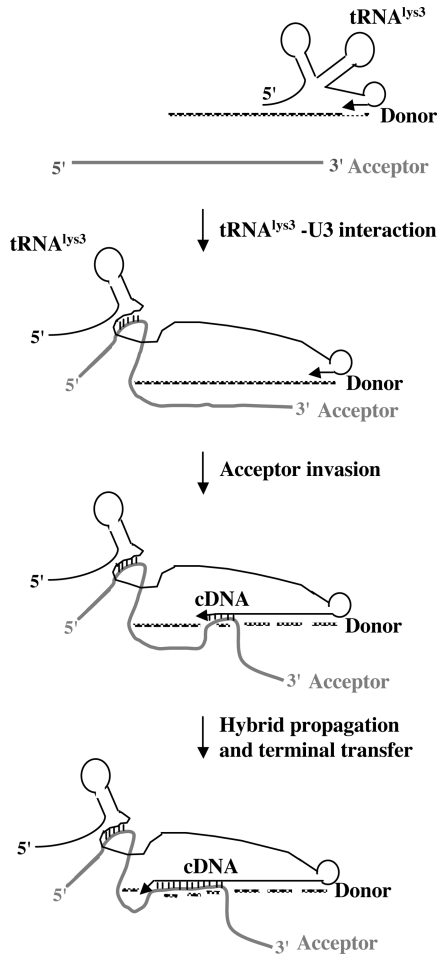

FIGURE 4: Proposed model for minus strand transfer that incorporates several mechanisms. Minus strand synthesis of HIV-1 is initiated when tRNA^{lys3} anneals to the PBS. The sequence complementarity between tRNA^{lys3} and U3 in the acceptor brings the acceptor 5′ terminus closer to the synthesized cDNA. As synthesis proceeds, the acceptor template invades the cDNA in the internal region of R. The acceptor−cDNA hybrid propagates from the invasion site toward the 5′ terminus of the acceptor template until the primer terminus switches from the donor to acceptor. The acceptor proximity effect and acceptor invasion-driven pathway cooperate to yield the maximal stimulation.

facilitates minus strand transfer, a DNA primer P1, which was of exactly the same sequence as tRNA^{lys3}, was prepared. Presumably, DNA primer P1 could interact with acceptors A97h(−54) and mat-A97h(−54) via sequence complementarity. Moreover, any differences in the folding of P1 compared to tRNA^{lys3} would lead to primer−acceptor interactions of different stability, ultimately resulting in a different transfer efficiency. Also, as a control, a second DNA primer P2, which represented the first 18 nt of the 3′ terminus of tRNA^{lys3} and was complementary to only PBS on the donor, was designed. Compared to primer P1, P2 was not capable of interacting with the U3 sequences in the acceptor RNA. Three acceptor templates A97h, A97h(−54), and mat-A97h(−54), were utilized in this study (Figure 3A).

Transfer profiles of each transfer reaction are presented in a graph showing time dependence in Figure 3D, and the final efficiencies of each transfer reaction are summarized in Figure 3E. When using DNA primer P1 with D520, no differences between results with different acceptors were observed. Since the presence of acceptor A97h already promoted a transfer efficiency of ∼78%, any possible small increases in transfer efficiency with either A97h(−54) or mat-A97h(−54) that resulted from P1−U3 interaction might be hard to detect. For D199, however, we observed transfer efficiencies of ∼42% with A97h, ∼44% with A97h(−54), and ∼43% with mat-A97h(−54). Clearly, the presence of P1−U3 interaction conferred by A97h(−54) and mat-A97h(−54) had no significant effect on the transfer reaction of D199. Also, for all three acceptors used in this experiment, there was no great difference in transfer when using P1 as opposed to using P2. Evidently, although P1 possesses the sequence available for interacting with U3, P1 cannot interact with U3 in a way that greatly improves transfer like tRNA^{lys3}.

DISCUSSION

Previously, we designed a reconstituted system in vitro to simulate HIV-1 minus strand transfer. In a DNA-primed transfer reaction, donor RNA template D199 promoted a transfer efficiency of ∼35% with acceptor RNA template A97h. Later, an approximately 2-fold increase in transfer efficiency was observed when using donor template D520 under the same reaction conditions. This result demonstrated that donor RNA sequences 3′ to the PBS influence transfer efficiency. Examination of the effect of homology on transfer and the acceptor RNase H cleavage profile suggested that both D199 and D520 promoted transfer mainly through an acceptor invasion-driven pathway. In this pathway, an initial acceptor−cDNA contact at an invasion site spreads to complete terminus transfer of the cDNA. However, by comparing the significance of each transfer step acceptor invasion, hybrid propagation, and terminal transfer involved in these two donor systems, we presented evidence that for D520, efficient acceptor invasion increased the local concentration of the region of the acceptor complementary to the cDNA primer terminus, stimulating more efficient transfer through an acceptor proximity effect (*23, 24*).

The facts that a nonanucleotide segment in the Mal strain of HIV-1 could interact with tRNA^{lys3} to stimulate minus strand transfer and that this nonanucleotide segment is conserved throughout different strains of the HIV-1 genome suggest that the segment has an important role (*56*). These observations prompted us to examine whether introduction of the tRNA^{lys3}−U3 interaction could overcome defects involved with inefficient invasion-driven transfer from D199, leading to more efficient overall transfer. Also, we wanted to test whether the tRNA^{lys3}−U3 interaction would promote transfer of D520 to an even higher efficiency. The substrates utilized by Marquet and co-workers included a donor template, which represented the first 311 nt of the 5′ terminus of the viral genome, and an acceptor template, which represented the first 639 nt of the 3′ terminus of the viral genome (*56*). This transfer system allowed the acceptor invasion-driven pathway and tRNA^{lys3}−U3 interaction. However, the donor template used in this system was 209 nt shorter at the 3′ end than donor template D520 used in our study. The tRNA^{lys3}-primed transfer system of D520 would give us a model in which the stimulatory effect on transfer conferred by a long genomic sequence 3′ of PBS (*23*) was also included.

To examine the effect of the tRNA^{lys3}−U3 interaction on the minus strand transfer reaction of D199 and D520, we prepared A97h(−54), an acceptor not only capable of

facilitating invasion-driven transfer similar to A97h but also capable of interacting with $tRNA^{lys3}$ by means of its nonanucleotide sequence complementarity. In $tRNA^{lys3}$-primed reactions, with both donors, a significant stimulation in the transfer reaction was observed using A97h(−54) compared to using A97h. Differences in transfer efficiency between the two donors were reduced when using A97h(−54) compared to using A97h. Also, the specific absence of $tRNA^{lys3}$−U3 interaction in the longer acceptor, achieved by using either Δ-A97h(−54) or mut-A97h(−54), led to a significant decrease in transfer efficiency for both of the donor systems, an observation consistent with the mutational study performed by the Marquet group (*56*). We interpret these results to mean that the $tRNA^{lys3}$−U3 interaction compensated for the inefficient acceptor invasion-driven pathway exhibited by D199, greatly facilitating transfer to 78% by increasing the local concentration of acceptor, and further promoted D520 to reach a higher transfer efficiency of 85%.

$tRNA^{lys3}$-primed D199 promoted transfer at an efficiency of 18% with A97h, while this number increased greatly to 78% with A97h(−54). Could this have meant that $tRNA^{lys3}$−U3 interaction is sufficient for the achievement of maximal stimulation? To answer this question meaningfully, we measured the stimulatory ability of the $tRNA^{lys3}$−U3 interaction with a substrate that does not support invasion-driven transfer, A19h(−54). For both D520 and D199, a decrease in transfer efficiency was observed when utilizing A19h(−54) compared to utilizing A97h(−54). Such a decrease was more significant with D199. Evidently, whether the acceptor invasion reaction is occurring with high efficiency, the proximity effect through $tRNA^{lys3}$−U3 interaction needs the assistance of acceptor invasion occurring early in the transfer reaction to achieve maximal stimulation.

To examine whether an alternative $tRNA^{lys3}$−U3 interaction with sequence complementarity at different positions could also promote transfer as efficiently as the $tRNA^{lys3}$−U3 interaction identified by the Marquet group (*56*), acceptor template mat-A97h(−54) was generated. The fact that mat-A97h(−54) promoted transfer just as efficiently as A97h(−54) indicates that the $tRNA^{lys3}$−U3 interaction, which facilitates more efficient transfer, is not restricted to the wild-type viral sequence but could be achieved through complementary mutations. Also, to analyze whether just sequence complementary between the primer and U3 in the acceptor is sufficient to stimulate minus strand transfer or whether proper folding of $tRNA^{lys3}$ is also essential for the reaction, the DNA primer P1 was designed. The potential P1−U3 interaction did not improve the transfer reaction of D199, suggesting that proper folding of the primer is required for effective primer−U3 interaction.

It is worth noting that DNA primer P2 is complementary to only the PBS in the viral genome and is the same primer utilized to initiate minus strand DNA synthesis in our previous studies (*23, 24*). In the P2-primed transfer reaction with A97h, the transfer efficiency was ∼75% for D520 and ∼35% for D199 (Figure 3E). In the $tRNA^{lys3}$-primed transfer reaction with A97h, however, the transfer efficiency was only ∼40% for D520 and ∼18% for D199 (Figure 1C). Clearly, DNA primer P2 promoted more efficient transfer than the $tRNA^{lys3}$ primer. One possible explanation is that in the absence of $tRNA^{lys3}$−U3 interaction with A97h, the $tRNA^{lys3}$ primer is in a conformation that is not entirely favorable for acceptor invasion-initiated transfer.

Previously, when using acceptors of a bipartite structure which allowed acceptor invasion and terminal transfer but not hybrid propagation, we observed that blockage of hybrid propagation did not have a strong effect on the transfer reaction with D520. We interpreted this result to mean that efficient acceptor invasion in the D520 system raises the local concentration of the 5′ terminus of the acceptor complementary to the cDNA 3′ terminus and promotes transfer via an acceptor proximity effect. The results imply that invasion can stimulate terminus transfers by two parallel acting mechanisms. It would promote branch migration of the RNA−DNA hybrid formed at the invasion site until the hybrid expanded to the cDNA terminus to complete transfer. Alternatively, the binding of the acceptor at the invasion site would promote terminus transfer by proximity (*24*). In this study, the stimulation of transfer observed with the $tRNA^{lys3}$−U3 interaction indicates that $tRNA^{lys3}$−U3 interaction brings the acceptor and elongated primer into proximity. In other previous work, a stimulation of transfer was also observed in a substrate system in which both the donor and acceptor RNAs harbored the functional motif dimerization initiation site (DIS). DIS were shown to adhere the two templates (*63*−*65*), again increasing the local concentration. The interaction was proposed to form the basis of the higher transfer efficiency (*66, 67*). Overall, these observations suggest that an acceptor proximity effect can be utilized by HIV-1 in several ways to promote transfer. Proximity can be achieved by either a tRNA−template interaction, a template−cDNA invasion (*24*), or a template−template hairpin kissing process as in DIS (*24, 66, 67*).

On the basis of our current results, we propose that multiple mechanisms work together in successive steps to achieve efficient minus strand transfer of HIV-1 (Figure 4). The reaction is initiated by a $tRNA^{lys3}$ primer annealed to the PBS (*68, 69*). The sequence complementarity between $tRNA^{lys3}$ and U3 in the acceptor brings the acceptor 5′ terminus closer to the primer−donor complex. As synthesis proceeds, the acceptor invades the synthesized cDNA in the internal region of R, facilitating the acceptor 3′ terminus to anneal to the elongated primer−donor complex at the invasion site. The acceptor−cDNA hybrid propagates, by branch migration or proximity interactions, from the invasion site to the 5′ terminus of the acceptor until transfer is completed (*20, 21, 23, 24*). Presumably, this complex, multistep process has evolved because highly efficient −sssDNA transfer has been critical for the long-term survival of HIV-1.

ACKNOWLEDGMENT

We thank Dr. Dorota Piekna-Przybylska, Jason Stewart, Sean Rigby, and Wen Shen for helpful discussions and critical reading of the manuscript.

REFERENCES

1. Baltimore, D. (1970) RNA-dependent DNA polymerase in virions of RNA tumour viruses. *Nature 226*, 1209–1211.
2. Temin, H. M., and Mizutani, S. (1970) RNA-dependent DNA polymerase in virions of Rous sarcoma virus. *Nature 226*, 1211–1213.

3. Telesnitsky, A., and Goff, S. P. (1993) Strong-stop Strand Transfer during Reverse Transcription. In *Reverse Transcriptase* (Skalka, A. M., and Goff, S. P., Eds.) pp 49−83, Cold Spring Harbor Laboratory Press, Plainview, NY.
4. Telesnitsky, A., and Goff, S. P. (1997) Reverse Transcription and the Generation of Retroviral DNA. In *Retroviruses* (Coffin, J. M., Hughes, S. H., and Varmus, H. E., Eds.) pp 121−160, Cold Spring Harbor Labortatory Press, Plainview, NY.
5. Levin, J. G., Guo, J., Rouzina, I., and Musier-Forsyth, K. (2005) Nucleic acid chaperone activity of HIV-1 nucleocapsid protein: Critical role in reverse transcription and molecular mechanism. *Prog. Nucleic Acid Res. Mol. Biol. 80*, 217–286.
6. Rein, A., Henderson, L. E., and Levin, J. G. (1998) Nucleic-acid-chaperone activity of retroviral nucleocapsid proteins: Significance for viral replication. *Trends Biochem. Sci. 23*, 297–301.
7. Cristofari, G., and Darlix, J. L. (2002) The ubiquitous nature of RNA chaperone proteins. *Prog. Nucleic Acid Res. Mol. Biol. 72*, 223–268.
8. Guo, J., Wu, T., Anderson, J., Kane, B. F., Johnson, D. G., Gorelick, R. J., Henderson, L. E., and Levin, J. G. (2000) Zinc finger structures in the human immunodeficiency virus type 1 nucleocapsid protein facilitate efficient minus- and plus-strand transfer. *J. Virol. 74*, 8980–8988.
9. Guo, J., Wu, T., Kane, B. F., Johnson, D. G., Henderson, L. E., Gorelick, R. J., and Levin, J. G. (2002) Subtle alterations of the native zinc finger structures have dramatic effects on the nucleic acid chaperone activity of human immunodeficiency virus type 1 nucleocapsid protein. *J. Virol. 76*, 4370–4378.
10. Lapadat-Tapolsky, M., Gabus, C., Rau, M., and Darlix, J. L. (1997) Possible roles of HIV-1 nucleocapsid protein in the specificity of proviral DNA synthesis and in its variability. *J. Mol. Biol. 268*, 250–260.
11. Hong, M. K., Harbron, E. J., O'Connor, D. B., Guo, J., Barbara, P. F., Levin, J. G., and Musier-Forsyth, K. (2003) Nucleic acid conformational changes essential for HIV-1 nucleocapsid protein-mediated inhibition of self-priming in minus-strand transfer. *J. Mol. Biol. 325*, 1–10.
12. You, J. C., and McHenry, C. S. (1994) Human immunodeficiency virus nucleocapsid protein accelerates strand transfer of the terminally redundant sequences involved in reverse transcription. *J. Biol. Chem. 269*, 31491–31495.
13. Driscoll, M. D., Golinelli, M. P., and Hughes, S. H. (2001) In vitro analysis of human immunodeficiency virus type 1 minus-strand strong-stop DNA synthesis and genomic RNA processing. *J. Virol. 75*, 672–686.
14. Driscoll, M. D., and Hughes, S. H. (2000) Human immunodeficiency virus type 1 nucleocapsid protein can prevent self-priming of minus-strand strong stop DNA by promoting the annealing of short oligonucleotides to hairpin sequences. *J. Virol. 74*, 8785–8792.
15. Guo, J., Henderson, L. E., Bess, J., Kane, B., and Levin, J. G. (1997) Human immunodeficiency virus type 1 nucleocapsid protein promotes efficient strand transfer and specific viral DNA synthesis by inhibiting TAR-dependent self-priming from minus-strand strong-stop DNA. *J. Virol. 71*, 5178–5188.
16. Peliska, J. A., Balasubramanian, S., Giedroc, D. P., and Benkovic, S. J. (1994) Recombinant HIV-1 nucleocapsid protein accelerates HIV-1 reverse transcriptase catalyzed DNA strand transfer reactions and modulates RNase H activity. *Biochemistry 33*, 13817–13823.
17. Heilman-Miller, S. L., Wu, T., and Levin, J. G. (2004) Alteration of nucleic acid structure and stability modulates the efficiency of minus-strand transfer mediated by the HIV-1 nucleocapsid protein. *J. Biol. Chem. 279*, 44154–44165.
18. Garces, J., and Wittek, R. (1991) Reverse-transcriptase-associated RNaseH activity mediates template switching during reverse transcription in vitro. *Proc. Biol. Sci. 243*, 235–239.
19. Gopalakrishnan, V., Peliska, J. A., and Benkovic, S. J. (1992) Human immunodeficiency virus type 1 reverse transcriptase: Spatial and temporal relationship between the polymerase and RNase H activities. *Proc. Natl. Acad. Sci. U.S.A. 89*, 10763–10767.
20. Chen, Y., Balakrishnan, M., Roques, B. P., and Bambara, R. A. (2003) Steps of the acceptor invasion mechanism for HIV-1 minus strand strong stop transfer. *J. Biol. Chem. 278*, 38368–38375.
21. Chen, Y., Balakrishnan, M., Roques, B. P., and Bambara, R. A. (2005) Acceptor RNA cleavage profile supports an invasion mechanism for HIV-1 minus strand transfer. *J. Biol. Chem. 280*, 14443–14452.
22. Chen, Y., Balakrishnan, M., Roques, B. P., Fay, P. J., and Bambara, R. A. (2003) Mechanism of minus strand strong stop transfer in HIV-1 reverse transcription. *J. Biol. Chem. 278*, 8006–8017.
23. Song, M., Balakrishnan, M., Chen, Y., Roques, B. P., and Bambara, R. A. (2006) Stimulation of HIV-1 minus strand strong stop DNA transfer by genomic sequences 3′ of the primer binding site. *J. Biol. Chem. 281*, 24227–24235.
24. Song, M., Basu, V. P., Hanson, M. N., Roques, B. P., and Bambara, R. A. (2008) Proximity and branch migration mechanisms in HIV-1 minus strand strong stop DNA transfer. *J. Biol. Chem. 283*, 3141–3150.
25. Wisniewski, M., Balakrishnan, M., Palaniappan, C., Fay, P. J., and Bambara, R. A. (2000) The sequential mechanism of HIV reverse transcriptase RNase H. *J. Biol. Chem. 275*, 37664–37671.
26. Palaniappan, C., Wisniewski, M., Wu, W., Fay, P. J., and Bambara, R. A. (1996) Misincorporation by HIV-1 reverse transcriptase promotes recombination via strand transfer synthesis. *J. Biol. Chem. 271*, 22331–22338.
27. DeStefano, J. J., Mallaber, L. M., Fay, P. J., and Bambara, R. A. (1993) Determinants of the RNase H cleavage specificity of human immunodeficiency virus reverse transcriptase. *Nucleic Acids Res. 21*, 4330–4338.
28. Peliska, J. A., and Benkovic, S. J. (1992) Mechanism of DNA strand transfer reactions catalyzed by HIV-1 reverse transcriptase. *Science 258*, 1112–1118.
29. Champoux, J. J. (1993) Roles of Ribonuclease in Reverse Transcription. In *Reverse Transcriptase* (Skalka, A. M., and Goff, S. P., Eds.) pp 103−117, Cold Spring Harbor Laboratory Press, Plainview, NY.
30. Negroni, M., and Buc, H. (2000) Copy-choice recombination by reverse transcriptases: Reshuffling of genetic markers mediated by RNA chaperones. *Proc. Natl. Acad. Sci. U.S.A. 97*, 6385–6390.
31. Lund, A. H., Duch, M., Lovmand, J., Jorgensen, P., and Pedersen, F. S. (1993) Mutated primer binding sites interacting with different tRNAs allow efficient murine leukemia virus replication. *J. Virol. 67*, 7125–7130.
32. Colicelli, J., and Goff, S. P. (1986) Isolation of a recombinant murine leukemia virus utilizing a new primer tRNA. *J. Virol. 57*, 37–45.
33. Kohlstaedt, L. A., and Steitz, T. A. (1992) Reverse transcriptase of human immunodeficiency virus can use either human tRNA(3Lys) or *Escherichia coli* tRNA(2Gln) as a primer in an in vitro primer-utilization assay. *Proc. Natl. Acad. Sci. U.S.A. 89*, 9652–9656.
34. Li, X., Mak, J., Arts, E. J., Gu, Z., Kleiman, L., Wainberg, M. A., and Parniak, M. A. (1994) Effects of alterations of primer-binding site sequences on human immunodeficiency virus type 1 replication. *J. Virol. 68*, 6198–6206.
35. Wakefield, J. K., Rhim, H., and Morrow, C. D. (1994) Minimal sequence requirements of a functional human immunodeficiency virus type 1 primer binding site. *J. Virol. 68*, 1605–1614.
36. Das, A. T., Klaver, B., and Berkhout, B. (1995) Reduced replication of human immunodeficiency virus type 1 mutants that use reverse transcription primers other than the natural tRNA(3Lys). *J. Virol. 69*, 3090–3097.
37. McCulley, A., and Morrow, C. D. (2007) Nucleotides within the anticodon stem are important for optimal use of tRNA(Lys,3) as the primer for HIV-1 reverse transcription. *Virology 364*, 169–177.
38. Aiyar, A., Cobrinik, D., Ge, Z., Kung, H. J., and Leis, J. (1992) Interaction between retroviral U5 RNA and the TψC loop of the tRNA(Trp) primer is required for efficient initiation of reverse transcription. *J. Virol. 66*, 2464–2472.
39. Arts, E. J., Li, X., Gu, Z., Kleiman, L., Parniak, M. A., and Wainberg, M. A. (1994) Comparison of deoxyoligonucleotide and tRNA(Lys-3) as primers in an endogenous human immunodeficiency virus-1 in vitro reverse transcription/template-switching reaction. *J. Biol. Chem. 269*, 14672–14680.
40. Wilhelm, M., Wilhelm, F. X., Keith, G., Agoutin, B., and Heyman, T. (1994) Yeast Ty1 retrotransposon: The minus-strand primer binding site and a cis-acting domain of the Ty1 RNA are both important for packaging of primer tRNA inside virus-like particles. *Nucleic Acids Res. 22*, 4560–4565.
41. Wakefield, J. K., Kang, S. M., and Morrow, C. D. (1996) Construction of a type 1 human immunodeficiency virus that maintains a primer binding site complementary to tRNA(His). *J. Virol. 70*, 966–975.
42. Kang, S. M., Zhang, Z., and Morrow, C. D. (1997) Identification of a sequence within U5 required for human immunodeficiency

virus type 1 to stably maintain a primer binding site complementary to tRNA(Met). *J. Virol. 71*, 207–217.
43. Zhang, Z., Kang, S. M., LeBlanc, A., Hajduk, S. L., and Morrow, C. D. (1996) Nucleotide sequences within the U5 region of the viral RNA genome are the major determinants for an human immunodeficiency virus type 1 to maintain a primer binding site complementary to tRNA(His). *Virology 226*, 306–317.
44. Li, Y., Zhang, Z., Wakefield, J. K., Kang, S. M., and Morrow, C. D. (1997) Nucleotide substitutions within U5 are critical for efficient reverse transcription of human immunodeficiency virus type 1 with a primer binding site complementary to tRNA(His). *J. Virol. 71*, 6315–6322.
45. Ni, N., Xu, W., and Morrow, C. D. (2007) Importance of A-loop complementarity with tRNAHis anticodon for continued selection of tRNAHis as the HIV reverse transcription primer. *Virol. J. 4*, 4.
46. Kang, S. M., and Morrow, C. D. (1999) Genetic analysis of a unique human immunodeficiency virus type 1 (HIV-1) with a primer binding site complementary to tRNAMet supports a role for U5-PBS stem-loop RNA structures in initiation of HIV-1 reverse transcription. *J. Virol. 73*, 1818–1827.
47. Skripkin, E., Isel, C., Marquet, R., Ehresmann, B., and Ehresmann, C. (1996) Psoralen crosslinking between human immunodeficiency virus type 1 RNA and primer tRNA3(Lys). *Nucleic Acids Res. 24*, 509–514.
48. Isel, C., Keith, G., Ehresmann, B., Ehresmann, C., and Marquet, R. (1998) Mutational analysis of the tRNA3Lys/HIV-1 RNA (primer/template) complex. *Nucleic Acids Res. 26*, 1198–1204.
49. Liang, C., Li, X., Rong, L., Inouye, P., Quan, Y., Kleiman, L., and Wainberg, M. A. (1997) The importance of the A-rich loop in human immunodeficiency virus type 1 reverse transcription and infectivity. *J. Virol. 71*, 5750–5757.
50. Wohrl, B. M., Ehresmann, B., Keith, G., and Le Grice, S. F. (1993) Nuclease footprinting of human immunodeficiency virus reverse transcriptase/tRNA(Lys-3) complexes. *J. Biol. Chem. 268*, 13617–13624.
51. Sarih-Cottin, L., Bordier, B., Musier-Forsyth, K., Andreola, M. L., Barr, P. J., and Litvak, S. (1992) Preferential interaction of human immunodeficiency virus reverse transcriptase with two regions of primer tRNA(Lys) as evidenced by footprinting studies and inhibition with synthetic oligoribonucleotides. *J. Mol. Biol. 226*, 1–6.
52. Barat, C., Lullien, V., Schatz, O., Keith, G., Nugeyre, M. T., Gruninger-Leitch, F., Barre-Sinoussi, F., LeGrice, S. F., and Darlix, J. L. (1989) HIV-1 reverse transcriptase specifically interacts with the anticodon domain of its cognate primer tRNA. *EMBO J. 8*, 3279–3285.
53. Andreola, M. L., Nevinsky, G. A., Barr, P. J., Sarih-Cottin, L., Bordier, B., Fournier, M., Litvak, S., and Tarrago-Litvak, L. (1992) Interaction of tRNALys with the p66/p66 form of HIV-1 reverse transcriptase stimulates DNA polymerase and ribonuclease H activities. *J. Biol. Chem. 267*, 19356–19362.
54. Li, X., Quan, Y., Arts, E. J., Li, Z., Preston, B. D., de Rocquigny, H., Roques, B. P., Darlix, J. L., Kleiman, L., Parniak, M. A., and Wainberg, M. A. (1996) Human immunodeficiency virus Type 1 nucleocapsid protein (NCp7) directs specific initiation of minus-strand DNA synthesis primed by human tRNA(Lys3) in vitro: Studies of viral RNA molecules mutated in regions that flank the primer binding site. *J. Virol. 70*, 4996–5004.
55. Isel, C., Marquet, R., Keith, G., Ehresmann, C., and Ehresmann, B. (1993) Modified nucleotides of tRNA(3Lys) modulate primer/template loop-loop interaction in the initiation complex of HIV-1 reverse transcription. *J. Biol. Chem. 268*, 25269–25272.
56. Brule, F., Bec, G., Keith, G., Le Grice, S. F., Roques, B. P., Ehresmann, B., Ehresmann, C., and Marquet, R. (2000) In vitro evidence for the interaction of tRNA(3)(Lys) with U3 during the first strand transfer of HIV-1 reverse transcription. *Nucleic Acids Res. 28*, 634–640.
57. Pandey, V. N., Kaushik, N., Rege, N., Sarafianos, S. G., Yadav, P. N., and Modak, M. J. (1996) Role of methionine 184 of human immunodeficiency virus type-1 reverse transcriptase in the polymerase function and fidelity of DNA synthesis. *Biochemistry 35*, 2168–2179.
58. Roda, R. H., Balakrishnan, M., Hanson, M. N., Wohrl, B. M., Le Grice, S. F., Roques, B. P., Gorelick, R. J., and Bambara, R. A. (2003) Role of the Reverse Transcriptase, Nucleocapsid Protein, and Template Structure in the Two-step Transfer Mechanism in Retroviral Recombination. *J. Biol. Chem. 278*, 31536–31546.
59. Morcock, D. R., Thomas, J. A., Sowder, R. C., II., Henderson, L. E., Crise, B. J., and Gorelick, R. J. (2008) HIV-1 inactivation by 4-vinylpyridine is enhanced by dissociating Zn^{2+} from nucleocapsid protein. *Virology 375*, 148–158.
60. Wu, W., Henderson, L. E., Copeland, T. D., Gorelick, R. J., Bosche, W. J., Rein, A., and Levin, J. G. (1996) Human immunodeficiency virus type 1 nucleocapsid protein reduces reverse transcriptase pausing at a secondary structure near the murine leukemia virus polypurine tract. *J. Virol. 70*, 7132–7142.
61. Wu, T., Guo, J., Bess, J., Henderson, L. E., and Levin, J. G. (1999) Molecular requirements for human immunodeficiency virus type 1 plus-strand transfer: Analysis in reconstituted and endogenous reverse transcription systems. *J. Virol. 73*, 4794–4805.
62. Isel, C., Ehresmann, C., Keith, G., Ehresmann, B., and Marquet, R. (1995) Initiation of reverse transcription of HIV-1: Secondary structure of the HIV-1 RNA/tRNA(3Lys) (template/primer). *J. Mol. Biol. 247*, 236–250.
63. Paillart, J. C., Marquet, R., Skripkin, E., Ehresmann, B., and Ehresmann, C. (1994) Mutational analysis of the bipartite dimer linkage structure of human immunodeficiency virus type 1 genomic RNA. *J. Biol. Chem. 269*, 27486–27493.
64. Paillart, J. C., Skripkin, E., Ehresmann, B., Ehresmann, C., and Marquet, R. (1996) A loop-loop "kissing" complex is the essential part of the dimer linkage of genomic HIV-1 RNA. *Proc. Natl. Acad. Sci. U.S.A. 93*, 5572–5577.
65. Skripkin, E., Paillart, J. C., Marquet, R., Ehresmann, B., and Ehresmann, C. (1994) Identification of the primary site of the human immunodeficiency virus type 1 RNA dimerization in vitro. *Proc. Natl. Acad. Sci. U.S.A. 91*, 4945–4949.
66. Balakrishnan, M., Fay, P. J., and Bambara, R. A. (2001) The kissing hairpin sequence promotes recombination within the HIV-I 5′ leader region. *J. Biol. Chem. 276*, 36482–36492.
67. Balakrishnan, M., Roques, B. P., Fay, P. J., and Bambara, R. A. (2003) Template Dimerization Promotes an Acceptor Invasion-Induced Transfer Mechanism during Human Immunodeficiency Virus Type 1 minus-Strand Synthesis. *J. Virol. 77*, 4710–4721.
68. Mak, J., Khorchid, A., Cao, Q., Huang, Y., Lowy, I., Parniak, M. A., Prasad, V. R., Wainberg, M. A., and Kleiman, L. (1997) Effects of mutations in Pr160gag-pol upon tRNA(Lys3) and Pr160gag-plo incorporation into HIV-1. *J. Mol. Biol. 265*, 419–431.
69. Marquet, R., Isel, C., Ehresmann, C., and Ehresmann, B. (1995) tRNAs as primer of reverse transcriptases. *Biochimie 77*, 113–124.

BI802149J